Foundations of Classical Control Theory with Reference to Eigenvalue Geometry

by THOMAS R. KURFESS *and* MARK L. NAGURKA

Department of Mechanical Engineering, Carnegie Mellon University, Pittsburgh, PA 15213, U.S.A.

ABSTRACT: *The foundations of linear time-invariant control are re-examined via a new geometric paradigm, gain plots. These plots depict eigenvalue trajectory as an explicit function of gain. Various classical control concepts are generalized in nine theorems and demonstrated in three simple, yet pedagogical, examples.*

I. Introduction

There have been many important developments in classical control theory of linear time-invariant (LTI) systems as a result of geometric perspectives (1–3). These graphical methods remain key control analysis and design tools even in the post-computer age. In fact, the advent of the computer has extended these methods considerably. For example, multivariable root locus plots can be generated as readily as single-input, single-output (SISO) root locus plots. The power and availability of software tools has prompted us to consider a new geometric perspective of the Evans root locus. The resulting plots, called gain plots, show the explicit variation of eigenvalue magnitudes and angles with respect to a scalar system parameter, such as forward gain (4). The eigenvalue magnitude vs gain is portrayed in a magnitude gain plot using a log–log scale and the eigenvalue angle vs gain is displayed in an angle gain plot using a semi-log scale (with the logarithms being base 10). Although we select gain as the variable of interest, it should be noted that any parameter may be used in the geometric analysis.

In this paper we employ the standard state-space representation of an LTI system:

$$\dot{x}(t) = Ax(t) + Bu(t) \qquad (1)$$

$$y(t) = Cx(t) + Du(t), \qquad (2)$$

where $x \in \mathcal{R}_n$ is the state, $u \in \mathcal{R}_m$ is the plant command or control input, $y \in \mathcal{R}_m$ is the plant output and $\{A, B, C, D\} \in \mathcal{R}$ with appropriate dimensions. The input–output dynamics are governed by a square transfer function matrix, $G(s)$:

$$G(s) = C[sI - A]^{-1}B + D. \qquad (3)$$

The system is embedded in a unity feedback closed-loop configuration with forward static compensator, kI, implying that each input channel is scaled by the same

constant gain, k. (Note that the plant transfer function matrix and any dynamic compensation may be combined in the transfer function matrix $\mathbf{G}(s)$.) The control law is given by

$$\mathbf{u}(t) = k\mathbf{I}\mathbf{e}(t), \tag{4}$$

where

$$\mathbf{e}(t) = \mathbf{r}(t) - \mathbf{y}(t) \tag{5}$$

is the error and $\mathbf{r}(t) \in \mathcal{R}_m$ is the reference (command) signal that $\mathbf{y}(t)$ must track. The closed-loop transfer function matrix is

$$\mathbf{G}_{CL}(s) = [\mathbf{I} + k\mathbf{G}(s)]^{-1} k\mathbf{G}(s). \tag{6}$$

To develop the root locus plot, the migration of the eigenvalues of $\mathbf{G}_{CL}(s)$ in the complex plane is portrayed for $0 \leqslant k < \infty$. The eigenvalues of the closed-loop system, $s = \lambda_i \, (i = 1, 2, \ldots, n)$, are the roots of $\phi_{CL}(s)$, the closed-loop characteristic polynomial:

$$\phi_{CL}(s) = \phi_{OL}(s) \det [\mathbf{I} + k\mathbf{G}(s)], \tag{7}$$

where $\phi_{OL}(s)$ is the open-loop characteristic polynomial:

$$\phi_{OL}(s) = \det [s\mathbf{I} - \mathbf{A}]. \tag{8}$$

The roots of (8) are the open-loop poles; they are also the eigenvalues of $\mathbf{A}$. By equating the determinant in (7) to zero, the multiple-input, multiple-output (MIMO) generalization of the SISO characteristic equation $(1 + kg(s) = 0)$ is obtained. The presence of the determinant is the major challenge in generalizing the SISO root locus sketching rules to MIMO systems and complicates the root locus plot. For example, the root locus branches "move" between several copies (Riemann sheets) in the s-plane that are connected at singularity points known as branch points (5, 6).

Although it is not normally possible to sketch MIMO root loci by inspection, the closed-loop system eigenvalues may be computed numerically from

$$\lambda_i = \text{eig}\,[\mathbf{A} - \mathbf{B}(\mathbf{I} + k\mathbf{D})^{-1} k\mathbf{C}], \quad i = 1, 2, \ldots, n, \tag{9}$$

where eig $[\mathbf{Q}]$ represents the eigenvalues of matrix $\mathbf{Q}$. In the examples, the loci of the eigenvalues are calculated from (9) as k is monotonically increased from zero.

II. Geometric Paradigms of Fundamental Control Concepts

This section presents a series of theorems that encapsulate fundamental concepts of classical control theory. Some of these concepts are discussed openly in the literature (7–9), while others do not seem to be mentioned. These theorems demonstrate the insight into control theory fundamentals provided by the gain plots.

We introduce two assumptions:

Assumption 1 : The systems analysed are lumped parameter LTI systems.
Assumption 2 : The forward scalar gain, k, is real and positive, i.e. $k \in \mathcal{R}$, $k > 0$.

Open-Loop eigenvalue representation

Theorem I

$$\lim_{k \to 0} R_i(k) = |\text{eig}(\mathbf{A})|, \quad i = 1, \ldots, n \tag{10}$$

$$\lim_{k \to 0} \theta_i(k) = \angle(\text{eig}(\mathbf{A})), \quad i = 1, \ldots, n, \tag{11}$$

where R_i and θ_i are the magnitude gain plot and angle gain plot ordinate values, respectively.

Proof : It follows from (7) that

$$\lim_{k \to 0} \phi_{\text{CL}}(s) = \lim_{k \to 0} \phi_{\text{OL}}(s) \det[\mathbf{I} + k\mathbf{G}(s)] = \phi_{\text{OL}}(s) \tag{12}$$

which is the open-loop case. ∎

Root locus 180° *criterion*

Theorem II
Lines in the angle gain plot must either lie on a multiple of $180°$ or must occur in a set of two segments that are symmetric about a multiple of $180°$.

Proof : Since $\{\mathbf{A}, \mathbf{B}, \mathbf{C}, \mathbf{D}\} \in \mathscr{R}$, then (9) represents the standard eigenvalue equation :

$$|\lambda I - (\mathbf{A} - \mathbf{B}(\mathbf{I} + k\mathbf{D})^{-1}k\mathbf{C})| = 0 \tag{13}$$

generating a polynomial in λ with real coefficients. Therefore, any complex eigenvalue must occur in a complex pair. ∎

High gain behavior of infinite magnitude eigenvalues
As k increases from 0 to ∞, the closed-loop eigenvalues trace out "root loci" in the complex plane. At zero gain, the eigenvalues of the closed-loop system are the open-loop poles. At infinite gain some of these eigenvalues approach finite transmission zeros, defined to be those values of z_i that satisfy the generalized eigenvalue problem :

$$\begin{bmatrix} z_i\mathbf{I} - \mathbf{A} & -\mathbf{B} \\ \mathbf{C} & \mathbf{D} \end{bmatrix} \begin{bmatrix} \mathbf{x}(0) \\ \mathbf{v} \end{bmatrix} = \begin{bmatrix} \mathbf{0} \\ \mathbf{0} \end{bmatrix}, \quad i = 1, 2, \ldots, m, \tag{14}$$

where $[\mathbf{x}(0)\ \mathbf{v}]^T$ is the right generalized eigenvector corresponding to the generalized eigenvalue, i.e. transmission zero, with $\mathbf{x}(0)$ representing the initial state and $\mathbf{v}$ being a vector representing input direction in the multi-input case. In the absence of pole/zero cancellation, the finite transmission zeros are the roots of the determinant of $\mathbf{G}(s)$. Algorithms have been developed for efficient and accurate computation of transmission zeros (10–12). Those eigenvalues that do not have matching zeros in the finite part of the s-plane are considered to have matching zeros at infinity ; these are the *infinite* eigenvalues. An interesting perspective of the high gain SISO root locus behavior is presented in (13).

Theorem III

For SISO systems with n poles and m transmission zeros:

$$\lim_{k \to \infty} \theta = \pm \frac{\pi(2i+1)}{n-m}, \quad i = 0, 1, \ldots, \tag{15}$$

where there are $n-m$ θ values corresponding to the $n-m$ infinite eigenvalues. This is the Butterworth configuration (14).

Theorem IV

For SISO systems with n poles and m transmission zeros:

$$\lim_{k \to \infty} R_i \propto k^{1/(n-m)}, \quad i = m+1, \ldots, n, \tag{16}$$

where there are $n-m$ magnitude values corresponding to $n-m$ infinite eigenvalues.

Proof: An LTI SISO system may be characterized by the transfer function

$$g(s) = \frac{n(s)}{d(s)} = \frac{\sum\limits_{i=0}^{m} b_i s^i}{\sum\limits_{j=0}^{n} a_j s^j}, \tag{17}$$

where $n(s)$ is the transfer function numerator of order m in s with coefficients, b_i $(i = 0, 1, \ldots, m)$, and $d(s)$ is the transfer function denominator of order n in s with coefficients, a_j $(j = 0, 1, \ldots, n)$ with $a_n = 1$. $\phi_{\mathrm{CL}}(s)$ is

$$\phi_{\mathrm{CL}}(s) = d(s) + kn(s) = \sum_{j=0}^{n} a_j s^j + k \sum_{i=0}^{m} b_i s^i \tag{18}$$

which can be written as

$$k = -\frac{d(s)}{n(s)} = -\frac{\sum\limits_{j=0}^{n} a_j s^j}{\sum\limits_{i=0}^{m} b_i s^i}. \tag{19}$$

From (19), as $k \to \infty$, the ratio of $d(s)$ to $n(s)$ must also tend towards infinity at the same rate. As $k \to \infty$, there are two possibilities for the magnitude ratio of $d(s)$ to $n(s)$, i.e.

$$n(s) \to 0 \tag{20}$$

and/or

$$d(s) \to \infty. \tag{21}$$

In the literature, it is shown that both of these criteria are satisfied as $k \to \infty$. For large gain, the highest order s term for both $d(s)$ and $n(s)$ dominates, since $|s| \to \infty$. Thus, in the limit as $k \to \infty$, (19) may be approximated by

$$k \cong -\frac{s^n}{b_m s^m} = -\frac{s^{n-m}}{b_m}. \tag{22}$$

From (22), the asymptotic behavior of the eigenvalues may be realized as

$$\lambda = s \cong -(b_m k)^{(1/n-m)}. \tag{23}$$

By taking the magnitude and angle of λ in (23), the proof for Theorems III and IV is completed. ∎

Eigenvalue approach rates to transmission zeros

Theorem V

For SISO systems with m transmission zeros

$$\lim_{k \to \infty} |z_i - \lambda_i| = k^{-1/w_i}, \quad i = 1, \ldots, m, \tag{24}$$

where w_i is the transmission zero multiplicity at z_i in the complex plane.

Before the proof is presented, we make the following assumption.

Assumption 3: There are no open-loop pole/zero cancelations. That is

$$p_j \neq z_i, \quad \forall \quad j, i, \tag{25}$$

where p_j and z_i are the poles and zeros of the system, respectively.

Proof : For (20) to hold:

$$\lim_{k \to \infty} \lambda_i = z_i, \quad i = 1, \ldots, m \tag{26}$$

since the z_is are the roots of $n(s)$.

Rewriting (19) as the ratio of products

$$k = -\frac{\prod\limits_{j=1}^{n} (s+p_j)}{\prod\limits_{i=1}^{m} (s+z_i)} \tag{27}$$

and evaluating it at

$$s = \lambda_i \to z_i \tag{28}$$

we recognize that $k \to \infty$, as (28) and consequently (20) are realized. Furthermore, since z_i are defined as the *finite* transmission zeros, $s - p_j$ must be finite, and $s - z_{i'} \neq 0$ (due to Assumption 3) if $z_i \neq z_{i'}$ where $i' \neq i$. In general, if there are w multiple poles at z_i:

$$\lim_{k \to \infty} \left[\frac{\prod\limits_{j=1}^{n} (s+p_j)}{\prod\limits_{i=1}^{m} (s+z_i)} \right]_{s=\lambda_i} = \lim_{\lambda_i \to z_i} \left[\frac{\prod\limits_{j=1}^{n} (s+p_j)}{\prod\limits_{i=1}^{m} (s+z_i)} \right]_{s=\lambda_i} \quad i = 1, \ldots, m \tag{29}$$

and

$$\lambda_i + p_j = \alpha_j, \quad i = 1, \ldots, m; j = 1, \ldots, n, \tag{30}$$

where α_j is a constant and

$$\lambda_i + z_{i'} = \beta_{i'}, \quad z_{i'} \neq z_i; i = 1, \ldots, m, \quad i' = 1, \ldots, m; i' \neq i, \tag{31}$$

where $\beta_{i'}$ is a constant.

Thus

$$\lim_{\lambda_i \to z_i} \left[\frac{\prod_{j=1}^{n} (s+p_j)}{\prod_{i=1}^{m} (s+z_i)} \right]_{s=\lambda_i} = \lim_{\lambda_i \to z_i} \left[\frac{A_i}{B_i (s+z_i)^w} \right]_{s=\lambda_i}, \quad i = 1, \ldots, m, \tag{32}$$

where

$$A_i = \prod_{j=1}^{n} \alpha_j \tag{33}$$

and

$$B_i = \prod_{\substack{i'=1 \\ i' \neq i \\ z_{i'} \neq z_i}}^{m} \beta_{i'} \tag{34}$$

completing the proof. ∎

Stability

Theorem VI
    If the principal angle of the closed-loop system eigenvalues is

$$0° \leqslant \theta < 360° \tag{35}$$

then the system is stable if

$$90° < \theta < 270°. \tag{36}$$

Outside this range, the system is unstable.

   Proof : Since the angle gain plot depicts the angle of the system eigenvalues, eigenvalues having angles in the range given by (36) are in the right-hand plane yielding unstable differential equations. This is the classical root locus stability criterion. ∎

Gain margin

Theorem VII
   For a given gain, k, the gain margin, GM, of the closed-loop system may be computed from the angle gain plot as

$$GM = 20 \log \left| \frac{k_s}{k} \right| \text{(dB)}, \tag{37}$$

where k_s is the gain corresponding to marginal stability.

Proof : In the frequency domain, GM (in dB) is defined as

$$GM = 20 \log |k_s(g(j\omega_a))| - 20 \log |k(g(j\omega_a))| = 20 \log \left| \frac{k_s(g(j\omega_a))}{k(g(j\omega_a))} \right|, \tag{38}$$

where

$$\angle g(j\omega_a) = -180°. \tag{39}$$

Equation (38) may be simplified as

$$GM = 20 \log \left(\left| \frac{k_s}{k} \right| \left| \frac{g(j\omega_a)}{g(j\omega_a)} \right| \right) = 20 \log \left| \frac{k_s}{k} \right|. \tag{40}$$

This ratio is the factor by which k may be varied before instability occurs. Both the numerator and denominator of (40) may be determined by inspection from the angle gain plot. ∎

Root sensitivity function

In classical control theory the root sensitivity, S_p, is defined as the relative change in the system roots or eigenvalues, $\lambda_i (i = 1, \ldots, n)$, with respect to a system parameter, p. Most often, the parameter analysed is the forward proportional controller gain. k. The root sensitivity with respect to gain is given by

$$S_k = \frac{d\lambda(k)/\lambda(k)}{dk/k} = \frac{d\lambda(k)}{dk} \frac{k}{\lambda(k)}. \tag{41}$$

Since the eigenvalues may occur as complex conjugate pairs, S_k may be complex.

Assumption 4 : There are no eigenvalues at the origin of the s-plane, i.e.

$$\lambda_i \neq 0, \quad \forall i = 1, \ldots, n. \tag{42}$$

However, the theorems are valid for eigenvalues arbitrarily close to the origin singularity. Based on these assumptions, we draw the following theorems.

Theorem VIII

The real component of the sensitivity function is given by

$$\text{Re}\{S_k\} = M_m, \tag{43}$$

where M_m is the slope of the loci in the magnitude gain plot.

Theorem IX

The imaginary component of the sensitivity function is given by

$$\text{Im}\{S_k\} = \frac{1}{\log e} M_a. \tag{44}$$

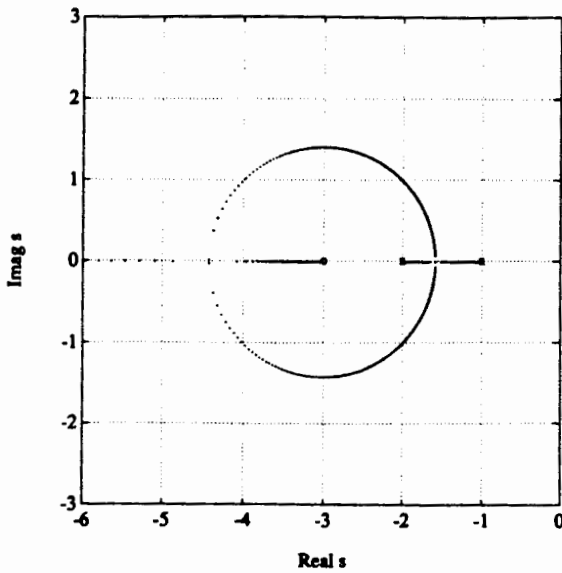where M_a is the slope of the loci in the angle gain plot.

FIG. 1. Root locus plot for Example 1.

Proof: Equation (41) may be rewritten (8, 15) in terms of the derivatives of natural logarithms as

$$S_k = \frac{d \ln (\lambda(k))}{d \ln (k)}.$$ (45)

The natural logarithm of the complex value, λ, may be written as the sum of the logarithm of the magnitude of λ and the angle of λ multiplied by $j = \sqrt{-1}$. Thus, (45) becomes

$$S_k = \frac{d \ln |\lambda(k)|}{d \ln (k)} + j \frac{d \angle \lambda(k)}{d \ln (k)} = \frac{d \log |\lambda(k)|}{d \log (k)} + j \frac{1}{\log e} \frac{d \angle \lambda(k)}{d \log (k)}.$$ (46)

The complex root sensitivity function is now expressed with distinct real and imaginary components employing the polar form of the eigenvalues. Since k is real and positive, d ln (k) and d log (k) are purely real, obviating the need to decompose those terms into polar form. (In general, most parameters studied are real and this proof is sufficient. If, however, the parameter analysed is complex, it is a straightforward task to extend the above analysis.) Equation (46) may be rewritten as

$$S_k = M_m + \frac{1}{\log e} M_a.$$ (47)

The proof is completed by taking the real and imaginary components of (47), yielding (43) and (44). It is interesting to note that the Cartesian representation of S_k is related to the polar representation of λ_i. ∎
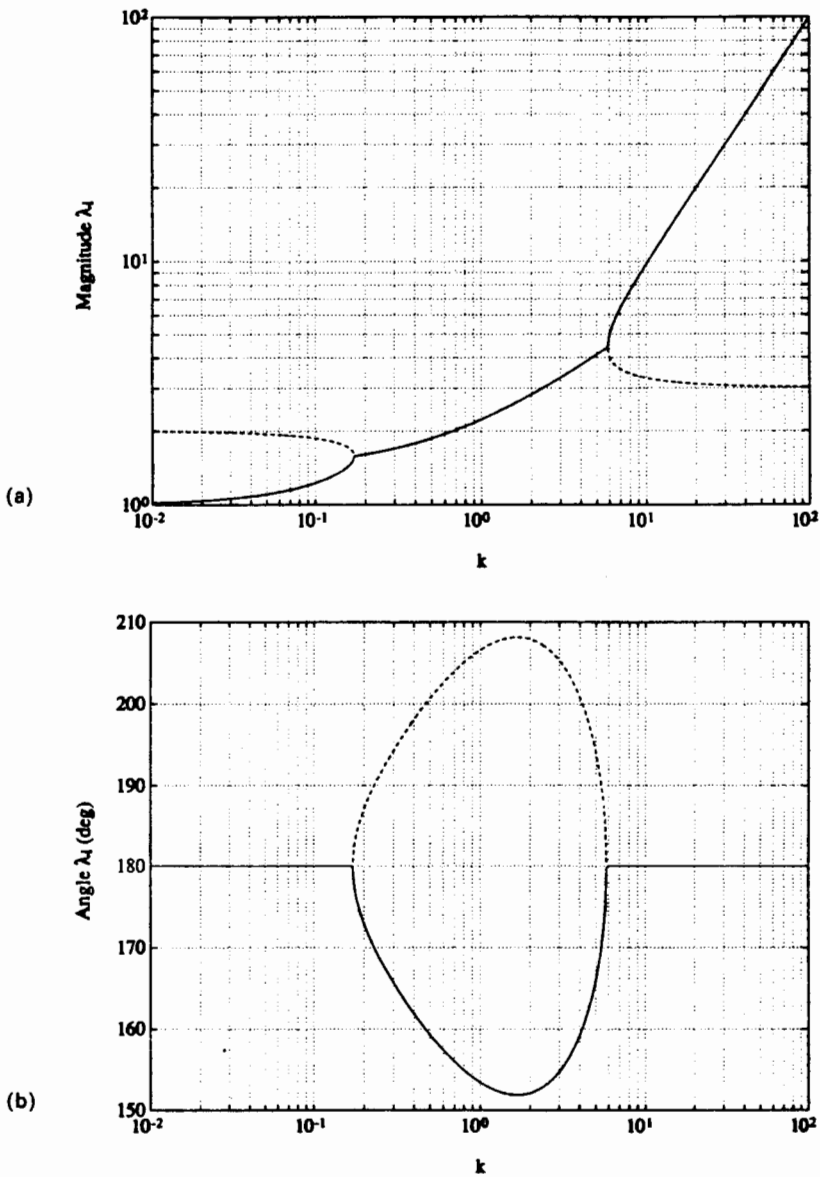
FIG. 2. (a) Magnitude gain plot for Example 1. (b) Angle gain plot for Example 1.

III. Examples

Example 1

To demonstrate the theorems presented above, we examine a second-order system with a PD controller:
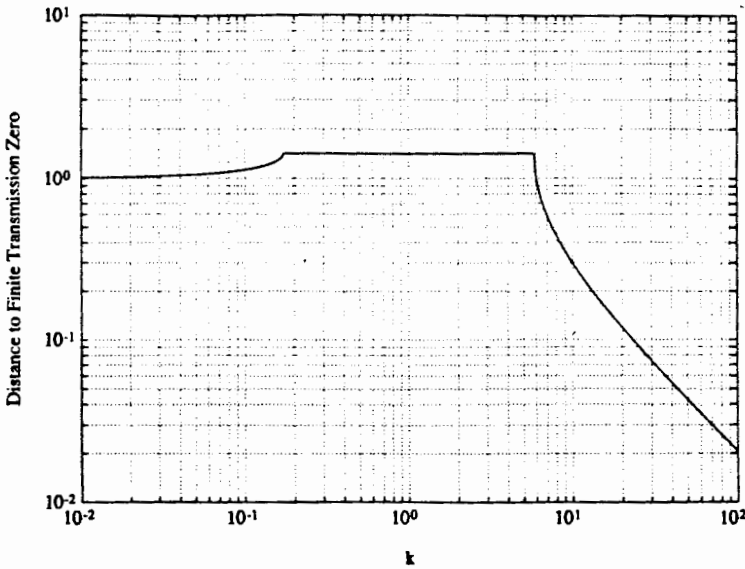
FIG. 3. Distance to single finite transmission zero for Example 1.

$$g_1(s) = \frac{s+3}{(s+1)(s+2)}. \tag{48}$$

The system has open-loop poles at $s = -1$, $s = -2$ and a finite transmission zero at $s = -3$. Hence, $n = 2$ and $m = 1$ in the notation employed earlier. The root locus of (48) is presented in Fig. 1. It shows a break-out point at $s \approx -1.6$, a break-in point at $s \approx -4.4$, Butterworth asymptotes along $-180°$, and reveals that the closed-loop system is stable given $\text{Re}(\lambda_i) < 0$, $\forall\ i,k$.

An alternate representation of Fig. 1 is the magnitude gain plot of Fig. 2(a) and the angle gain plot of Fig. 2(b). Here, the explicit influence of gain on the eigenvalue trajectories is represented. As $k \to 0$ the magnitude gain plot and angle gain plot reveal the influence on the magnitudes and angles, respectively, of the open-loop eigenvalues demonstrating Theorem I. The segments in the angle gain plot are either on the 180° line or symmetric about it, in agreement with Theorem II. Also, the break-out and break-in points are evident at $k \approx 0.17$ and $k \approx 5.83$, respectively. As $k \to \infty$ the angle gain plot shows the Butterworth configuration for a single infinite eigenvalue proceeding along a trajectory of 180° in accordance with Theorem III. Theorem IV is demonstrated by the corresponding high gain magnitude gain plot slope of unity for the infinite eigenvalue.

To observe the approach rate to the finite transmission zero, we have constructed a modified magnitude gain plot which shows the distance of the finite eigenvalue to the finite zero at $s = -3$. The resulting figure, Fig. 3, shows that as $k \to \infty$ the distance is inversely proportional to k confirming Theorem V for $w = 1$. Figure 3 also shows that between the break points there is a constant distance between the
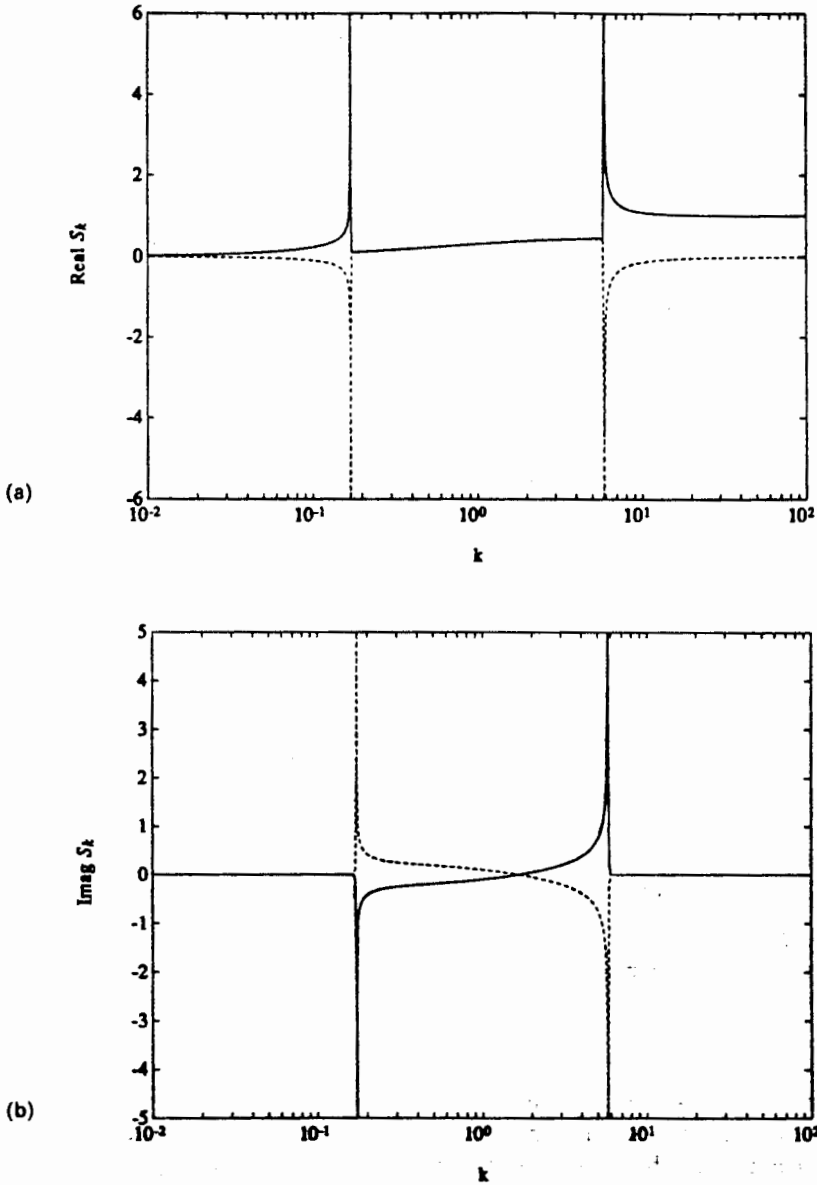
FIG. 4. (a) Real component of sensitivity for Example 1. (b) Imaginary component of sensitivity for Example 1.

eigenvalue and the transmission zero, demonstrating that the eigenvalue trajectory about the transmission zero is circular in the complex plane.

Since θ_i is always in the range prescribed by (36), the closed-loop system is stable for all gains, and hence has an infinite gain margin. A more interesting demonstration of Theorems VI and VII follows in Example 2.
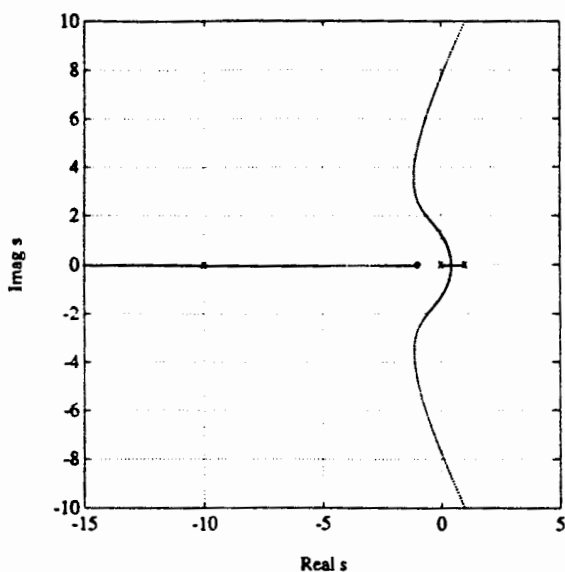
FIG. 5. Root locus plot for Example 2.

Theorems VIII and IX are demonstrated by the sensitivity plots of Fig. 4(a,b), respectively. (These figures were generated from (45) by plotting the real and imaginary components of S_k.) They clearly highlight the infinite sensitivities at the break points. Furthermore, they show the sensitivity function is real for $\lambda_i \in \mathscr{R}$. The crossover point at $k \approx 2$ in Fig. 4(b) corresponds to the extremum of $\text{Im}\{\lambda_i\}$. As $k \to \infty$ the finite eigenvalue becomes completely desensitized whereas the infinite eigenvalue has a sensitivity of unity, again confirming Theorems VIII and IX.

Example 2

This example (16) considers a third-order system employing PI control:

$$g_2(s) = \frac{s+1}{s(s-1)(s+10)^2}. \tag{49}$$

This system is open-loop unstable. The root locus plot of Fig. 5 shows that there is a regime for which the closed-loop system is stable. The corresponding gain plots are shown in Fig. 6(a), (b). It is possible using Theorem VI to determine the stable range as $132 < k < 1230$. From Theorem VII the gain margin can be computed at any design value of k. For example, at $k = 300$, the lower gain margin is $20 \log(132/300) \approx -7.1$ dB and the upper gain margin is $20 \log(1230/300) \approx 12.3$ dB.

Example 3

Here we consider the same system as in Example 2 with a PID controller:

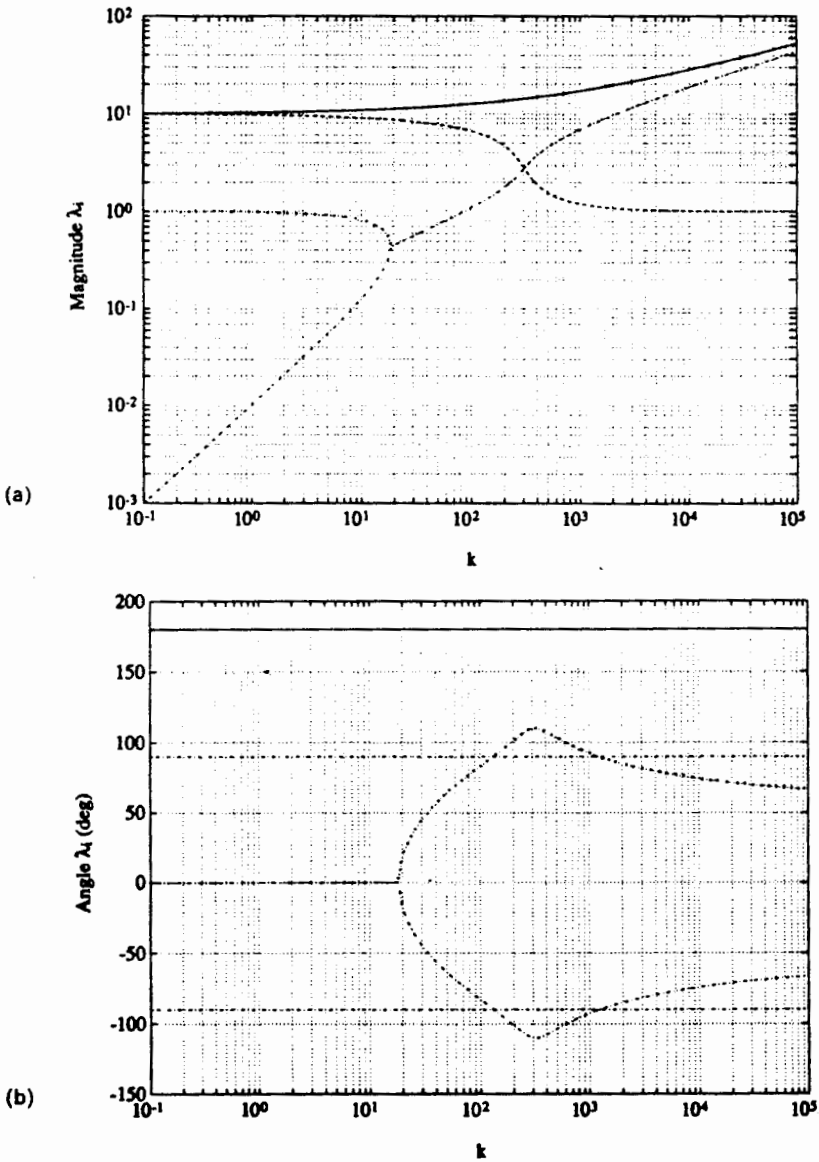$$g_3(s) = \frac{(s+1)^2}{s(s-1)(s+10)^2}. \tag{50}$$

FIG. 6. (a) Magnitude gain plot for Example 2. (b) Angle gain plot for Example 2.

The root locus plot is presented in Fig. 7 and shows the two finite eigenvalues approaching the double transmission zero at $s = -1$. As expected from Theorem V the approach rate to the double zeros is inversely proportional to $k^{1/2}$ since $w = 2$. This is demonstrated by the high gain slope of $-1/2$ in Fig. 8 which shows the distance to the finite transmission zeros.
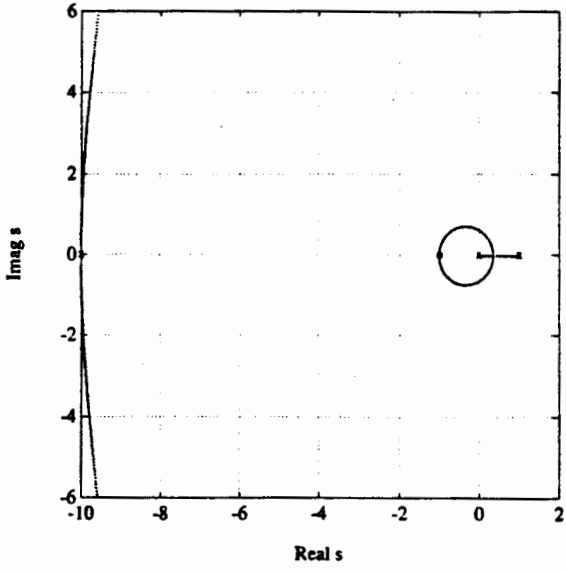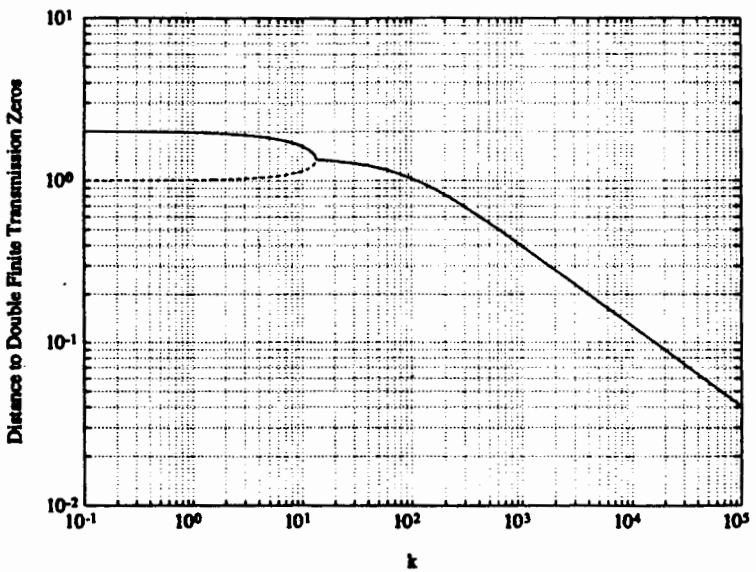
FIG. 7. Root locus plot for Example 3.

FIG. 8. Distance to double finite transmission zeros for Example 3.

IV. Conclusion

This paper has promoted the use of gain plots that expose closed-loop eigenvalue geometry as a function of a system parameter such as proportional gain. By

displaying the eigenvalue magnitude vs gain in a logarithmic plot and the eigenvalue angle vs gain in a semi-logarithmic plot, fundamental concepts of classical control can be determined by inspection. For example, stability, gain margin, root sensitivity, eigenvalue approach rates to both finite and infinite transmission zeros, as well as other properties are available. The gain plots embellish the information presented in the root locus, and are recommended as a supplementary tool for control system analysis and design.

Acknowledgement

References

(1) H. Nyquist, "Regeneration theory", *Bell Syst. Tech. J*, Vol. 11, pp. 126–147, 1932.

(2) H. W. Bode, "Relations between attenuation and phase in feedback amplifier design", *Bell Syst. Tech. J.*, Vol. 19, pp. 421–454, 1940.

(3) W. R. Evans, "Graphical analysis of control systems", *Trans. Am. Inst. Elec. Engrs*, Vol. 67, pp. 547–551, 1948.

(4) T. R. Kurfess and M. L. Nagurka, "Understanding the root locus using gain plots", *I.E.E.E. Control Syst. Mag.*, Vol. 11, No. 5, pp. 37–40, 1991.

(5) A. E. Yagle, "Properties of multivariable root loci", S. M. Thesis, Department of Electrical Engineering and Computer Science, Massachusetts Institute of Technology, Cambridge, MA, 1981.

(6) M. Athans, "Lecture notes on multivariable control systems: MIT subject 6.232", Massachusetts Institute of Technology, Cambridge, MA, 1982.

(7) R. C. Dorf, "Modern Control Systems", Sixth Edn, Addison-Wesley, Reading, MA, 1992.

(8) B. C. Kuo, "Automatic Control Systems", Fifth Edn, Prentice-Hall, Englewood Cliffs, NJ, 1991.

(9) K. Ogata, "Modern Control Engineering", Prentice-Hall, Englewood Cliffs, NJ, 1990.

(10) E. J. Davison and S. H. Wang, "Properties and calculation of transmission zeros of linear multivariable systems", *Automatica*, Vol. 10, pp. 643–658, 1974.

(11) A. J. Laub and B. C. Moore, "Calculation of transmission zeros using QZ techniques", *Automatica*, Vol. 14, pp. 557–566, 1978.

(12) D. Westreich, "Computing transfer function zeros of a state space system", *Int. J. Control*, Vol. 53, pp. 477–493, 1991.

(13) B. Friedland, "Control System Design", McGraw-Hill, New York, 1986.

(14) H. Kwakernaak and R. Sivan, "Linear Optimal Control Systems", Wiley-Interscience, New York, 1972.

(15) I. M. Horowitz, "Synthesis of Feedback Systems", Academic Press, New York, 1963.

(16) R. H. Cannon Jr, "Dynamics of Physical Systems", McGraw-Hill, New York, 1967.